

## Original Article

# Comprehensive circular RNA profiling reveals the regulatory role of circRNA\_0007694 in papillary thyroid carcinoma

Miao-Yun Long<sup>1\*</sup>, Jin-Wu Chen<sup>2\*</sup>, Yue Zhu<sup>1</sup>, Ding-Yuan Luo<sup>1</sup>, Shao-Jian Lin<sup>1</sup>, Xin-Zhi Peng<sup>1</sup>, Lang-Ping Tan<sup>1</sup>, Hong-Hao Li<sup>1</sup>

<sup>1</sup>Department of Thyroid Surgery, <sup>2</sup>Medical Examination Center, Sun Yat-sen Memorial Hospital, Sun Yat-sen University, Guangzhou 510000, China. \*Equal contributors.

Received August 29, 2019; Accepted February 2, 2020; Epub April 15, 2020; Published April 30, 2020

**Abstract:** Purpose: The present study aimed to identify differentially expressed circRNAs in thyroid cancer and verify their potential functions. Methods: Next-generation sequencing was used to identify differentially expressed circRNAs between papillary thyroid carcinoma (PTC) tissues and paired pericarcinomatous tissues. Polymerase chain reaction and Sanger sequencing methods successfully identified hsa\_circ\_0007694. A hsa\_circ\_0007694 over-expression vector was prepared to determine the effect of this circRNA on proliferation, migration, invasion, apoptosis, and the cell cycle in PTC cells. An *in vivo* animal assay was conducted by injecting PTC cells into the chests of mice. Further, RNA-seq was performed, followed by Gene Ontology and Kyoto Encyclopedia of Genes and Genomes (KEGG) analysis, to verify the regulatory mechanism of hsa\_circ\_0007694. Western blotting was used to verify the genes thought to be involved in the hsa\_circ\_0007694 regulatory pathways based on KEGG analysis. Results: We identified a circRNA, hsa\_circ\_0007694 that was down-regulated in PTC tissues compared to pericarcinomatous tissues. Over-expression of hsa\_circ\_0007694 promoted apoptosis and inhibited proliferation, migration, and invasion in PTC cells *in vitro*, and decreased tumor growth *in vivo*. Transcriptome sequence analysis suggested 129 differentially expressed genes between PTC tissue and paired pericarcinomatous tissue. KEGG analysis and western blotting indicated that the PI3K/AKT/mTOR and Wnt signaling networks are most likely to be related to hsa\_circ\_0007694 in thyroid cancer. Conclusion: The circRNA hsa\_circ\_0007694 is down-regulated in PTC and is therefore a potential therapeutic target.

**Keywords:** Papillary thyroid carcinoma, differential expressed circRNAs, hsa\_circ\_0007694, therapeutic target

## Introduction

Thyroid cancer is the most common tumor of the endocrine system, accounting for 2% of systemic malignancies and 95% of endocrine malignancies [1]. Furthermore, it is becoming more common year on year; the number of newly diagnosed thyroid cancer patients increased from 37,200 cases in 2009 to 63,000 cases in 2014, and the incidence rate increased from 4.9/100,000 in 1975 to 14.3/100,000 in 2009. Papillary thyroid carcinoma (PTC), which is a kind of differentiated thyroid cancer, accounts for about 90% thyroid cancer patients [2] and is almost entirely responsible for the aforementioned recent increase in the incidence of thyroid cancer. PTC grows slowly and

prognosis is generally good. However, its incidence and recurrence rate (20% to 40%) are high, and the mortality of PTC is about 50% of the total mortality of thyroid cancer [3]. In addition, PTC is set to be the third most common tumor in women in 2019, and national medical expenditure to treat it will reach 19 billion to 21 billion U.S. dollars, which will be a huge economic burden on families and society [2].

Currently, common methods of thyroid tumor diagnosis include clinical examination, thyroid radionuclide scanning, thyroid B ultrasound, and fine needle aspiration (FNA) [4]. Of these methods, FNA is considered the most important. However, FNA is only useful for cytological examination, and its success is directly related

to the experience of the practitioner and the amount of tissue obtained. A previous study reported that about 1/3 of thyroid malignancies can be missed using this method, resulting in adverse clinical diagnosis and treatment [5]. Furthermore, FNA is an invasive procedure, and patients consistently demonstrate low acceptance of this technique. With in-depth studies of tumor-related genes, knowledge of the molecular mechanism of PTC has improved. A previous study determined that mutations in *BRAF* and *RAS*, gene rearrangement of *RET*/PTC are related to the occurrence and invasiveness of PTC [6]. Of these genetic changes, *BRAF* mutation is most closely related to the occurrence and development of PTC. For example, *BRAF*<sup>V600E</sup> mutation is closely related to multifocal lymph node metastasis and high clinical pathological PTC staging, indicating poor tumor prognosis [7, 8]. However, the use of the *BRAF*<sup>V600E</sup> mutation as a diagnostic and prognostic marker has limitations. For instance, only 40% to 45% of PTC patients carry this gene mutation [7]. Therefore, the need for a new diagnostic biomarker for PTC patients is urgent.

Recent studies have shown that non-coding RNAs participate in chromatin modification and the regulation of transcription and gene expression [9, 10]. CircRNA is a class of non-coding RNA that is widely found in mammals. Unlike linear RNA, which has 5' and 3' ends, the closed circular structure of circRNA makes it more stable and therefore resistant to degradation by RNA exonucleases [11]. It has been reported that there is a link between circRNA and tumors, and a more comprehensive understanding of this relationship would promote our understanding of tumor pathogenesis. Zhang et al. reported abnormal differential expression of circRNAs between pancreatic ductal adenocarcinoma tissue and pericarcinomatous tissue using microarray technology [12]. Bachmayr-Heyda et al. revealed that the circRNA/paired linear RNA ratio is higher in colorectal cancer tissue than in normal colorectal tissue [13]. Wang et al. noted that the expression of hsa\_circ\_002059 in gastric cancer tissue was lower than that in pericarcinomatous tissue, and that this circRNA had high application value in clinical trials [14]. The evidence mentioned above indicates that circRNAs have the potential to be applied in cancer treatments. Although previous studies have laid a solid foundation for further study of this class of molecules, identifying

dysregulated circRNAs in thyroid cancer and elucidating their functions remains an ongoing process in the field of cancer research.

In the present study, differentially expressed circRNAs between PTC tissues and paired pericarcinomatous tissues were identified by circRNA sequencing. We further selected a specific circRNA (hsa\_circ\_0007694), which was down-regulated in cancer tissues, for subsequent analysis. Functionally, hsa\_circ\_0007694 inhibits HBT-101 and KHM-5M cell proliferation, migration, and invasion while suppressing apoptosis. The present study explored, for the first time, the function and mechanism of hsa\_circ\_0007694 in human thyroid cancer.

### Materials and methods

#### *Samples and H&E staining*

Fresh samples of PTC tissues (n=3, patients referred to as HA, WA, and LA) and paired pericarcinomatous tissues (n=3, HAP, WAP, LAP) were collected and each tissue was divided into two parts. One part was immediately transferred to liquid nitrogen and stored at -80°C until gDNA and total RNA extraction. Meanwhile, H&E staining was used to identify the pathological characteristics of the other part of the tissue. The final results were assessed by two experienced clinical technicians. Briefly, H&E staining was carried out as follows: 1) Samples were dewaxed with xylene for 10-15 min; 2) the xylene was washed away in an alcohol gradient; 3) samples were stained with hematoxylin dye for 15 min after immersion in distilled water for 5 min; 4) samples were immersed in hydrochloric acid for color separation for 20 s; 5) samples were immersed in distilled water for 10 min; 6) samples were soaked in 0.5% eosin for 20 s after washing; 7) samples were allowed to dry naturally, then gland packing sheet; and 8) a microscope was used to view the stained samples. This study was approved by the Human Research Ethics Committee of the Sun Yat-sen Memorial Hospital, Sun Yat-sen University.

#### *Sequencing*

Total RNA was used to deplete ribosomal RNA with a Ribo-Zero Gold Kit (Epicenter, USA). The rRNA-depleted RNAs were further incubated at 37°C for 1 h with 10 U/μg RNase R (Epicenter,

Madison, WI). The remaining RNAs were used to construct cDNA libraries according to the mRNA-seq Sample Preparation Kit protocol (Illumina, USA). A TruSeq PE Cluster Kit v3-cBot-HS (Illumina, USA) was used to form the sequence cluster according to the manufacturer's instructions. Then, 2×150 bp paired-end sequencing was carried out on an Illumina HiSeq2500 platform. Differential expression of circRNAs was identified according to a previous study [15]. An Illumina® TruSeq RNA Library Prep Kit v2 was used to construct RNA-seq libraries. RNA-seq data was treated according to the method of a previous study. Differentially expressed genes were identified. Enrichr (<http://amp.pharm.mssm.edu/Enrichr/>) was used to analyze Gene Ontology (GO) terms enriched in differentially expressed genes. The Enrichr settings used were described in a previous study [16]. Meanwhile, we used KOBAS software to test the statistical enrichment of differentially expressed genes in Kyoto Encyclopedia of Genes and Genomes (KEGG) pathways [17].

### *Identification of hsa\_circ\_007694*

Total RNA and gDNA was extracted from thyroid cancer tissues, pericarcinomatous tissues, BHT-101 cells, and KHM-5M cells with a MiniBEST Universal Genomic DNA Extraction Kit Ver.5.0 (Takara, Japan) and a MiniBEST Universal RNA Extraction Kit (Takara, Japan), respectively. The total RNA was subsequently reverse transcribed to cDNA with a PrimeScript™ II 1st Strand cDNA Synthesis Kit (Takara, Japan). The operation process was performed strictly according to the manufacturer's instructions. The concentration and quality of the total DNA and RNA were measured with a NanoDrop 8000 (Thermo Fisher, USA). Values of OD260/OD280 between 1.8 and 2.1 were considered to indicate ideal samples. The integrity of the DNA and RNA was analyzed by denaturing agarose gel. We designed two primer pairs to amplify hsa\_circ\_0007694 and the corresponding linear RNA. The primer sequences were as follows: hsa\_circ\_0007694 (forward): 5'-AGTACCATAGGCATCCTTCATCA-3', hsa\_circ\_0007694 (reverse): 5'-CCTCCACCTCCATTAGATTTCCA-3', linear RNA (forward): 5'-AGCCATTTGACCGTGGAGAA-3', linear RNA (reverse): 5'-TGGCTCTCTCCAGGTTTCGTT-3'. The reactions were performed in 20 µl volumes

comprising 10 µl 2× GoldStar Best MasterMix (Dye) (CWbiotech, China), 1 µl primer mixture (final concentration of each primer 0.5 pmol), 1 µl DNA template with different amounts of DNA, and 8 µl ddH<sub>2</sub>O. Thermal cycling conditions were as follows: 3 min at 98°C, followed by 40 cycles at 95°C for 15 s and 60°C for 25 s. The amplification products were further examined by agarose gel electrophoresis (2.0%) and Sanger sequencing. Meanwhile, we performed q-PCR analysis with different samples. The reaction conditions were similar to those used for PCR identification, but with minor modifications: the reactions were performed in 10 µl volumes comprising 5 µl 2× FastSYBR Mixture (CWbiotech, China), 0.5 µl primer mixture (final concentration of each primer 0.25 pmol), 1 µl DNA template with different amounts of DNA, and 3.5 µl ddH<sub>2</sub>O. Data were collected using an ABI analytical thermal cycler. RNA expression was calculated based on a relative standard curve using an  $\Delta\Delta\text{Ct}$  method, representing 10-fold dilutions of PCR products.

### *Cell treatment*

BHT-101 and KHM-5M cells were purchased from ATCC (Virginia, USA) and maintained in RPMI 1640 with 10% (v/v) FBS (Invitrogen, Carlsbad, CA). Cell lines were maintained in a humidified chamber in 5% CO<sub>2</sub> and at 37°C. A LV003 plasmid of hsa\_circ\_007694 was obtained from Genesee Biotech (China). A pEZ-LV003 vector was applied to construct a hsa\_circ\_007694 over-expression system. EndoFectin-Lenti™ and Titer Boost™ reagents were used to generate highly purified plasmids according to the standard protocol (FulenGen, Guangzhou, China). The lentiviral transfer vector was transfected into BHT-101 cells with a Lenti-Pac HIV Expression Packaging Kit (GeneCopoeia, USA).

### *Apoptosis, proliferation, and cell cycle*

Apoptosis of BHT-101 or KHM-5M cells treated with mock vehicle and BHT-101 or KHM-5M cells overexpressing hsa\_circ\_007694 was assessed with an Annexin V-FITC Apoptosis Detection Kit (Sigma Aldrich, USA). The operation process was performed strictly according to the manufacturer's instructions. Meanwhile, a cell proliferation assay of all of the various cells was carried out with an MTT kit (Sigma Aldrich, USA). OD values were measured after

24, 48, and 72 h. For a colony formation assay, 500 cells were placed into each well of a 6-well plate and maintained in media containing 10% FBS for 1 week. Colonies were fixed with methanol and stained with 0.1% crystal violet (Sigma Aldrich, USA) in PBS for 15 min. Colony formation was observed using an inverter microscope. In addition, flow cytometry was applied to analyze the cell cycle distribution of BHT-101 cells treated with mock vehicle and BHT-101 cells over-expressing hsa\_circ\_007694. After 48 h of transfection, cells were obtained via trypsin digestion treatment and fixed with 70% ethanol. A FACS calibur flow cytometer (BD Biosciences) was used to analyze cell cycle distribution.

### *Migration and invasion assay*

A cell migration assay was carried out with an EZCell™ Migration/Chemotaxis Assay Kit (Biovision, USA). Briefly, BHT-101 or KHM-5M cells treated with mock vehicle and BHT-101 or KHM-5M cells over-expressing hsa\_circ\_007694 were planted in the top chamber of each transwell ( $1 \times 10^6$  cells/ml, 100  $\mu$ l per chamber). Cells were cultured at 37°C for 24 h. Subsequently, cells that penetrated to the bottom membrane were fixed in methanol, stained with hematoxylin, and counted under an optical microscope. Cell invasion analysis was performed with an EZCell™ Cell Invasion Assay Kit (EZCell™, USA) according to the manuals supplied by the manufacturer. Briefly,  $1 \times 10^3$  BHT-101 or KHM-5M cells were seeded in 100  $\mu$ l serum-free media in the upper wells, which were coated with Matrigel basement extract. Cells were cultured at 37°C with 5% CO<sub>2</sub> for 24 h. Intact cells were removed, and migrated cells were fixed with 500  $\mu$ l cell dissociation solution/calcein-AM. Then, treated cells were incubated at 37°C in 5% CO<sub>2</sub> for 1 h and quantified by fluorimetric analysis.

### *In vivo nude mouse models*

Four-week-old female SPF/VAF nude mice weighing approximately 13 g were purchased from Vitalriver Company (Beijing, China). All of the animal experiments in the present study were approved by the Ethics Committee of Sun Yat-sen University. Then,  $3.5 \times 10^6$  BHT-101 cells treated with mock vehicle and  $3.5 \times 10^6$  BHT-101 cells over-expressing hsa\_circ\_007694 were injected into the armpit or rear flank of the

nude mice, respectively, to form implanted tumors (170  $\mu$ l RPMI1640 with 10% FBS). Tumor growth was monitored at six different time points. The tumor volume of both cells was recorded at the different time points. The mice were sacrificed 27 d after injection and the tumor tissues were obtained and weighed. The tumor specimens were immediately transferred to liquid nitrogen and stored at -80°C for further qPCR analysis.

### *Western blotting*

Cells were treated with pre-cooled cell lysate (volume of PMSF: volume of RIPA cell lysate = 1:100). A BCA Protein Assay Kit (Beyotime, P0011) was used to determine the protein concentration. After boiling with SDS-PAGE sample buffer for 5 min, SDS-PAGE was performed. Then, the proteins were transferred onto a polyvinylidene difluoride membrane (Millipore, USA). After blocking for 1 h at room temperature, the membrane was incubated with rabbit polyclonal anti-mouse p21 (1:400), p-GSK3B (1:1000), GSK3B (1:500), VIM (1:500), p-AKT (1:1000), AKT (1:1000), N-CAD (1:500), and p53 (1:2000) antibodies (BOSTER, USA) overnight. Before detection with an ECL Chemiluminescence Detection Kit (Beyotime Institute of Biotechnology, China), proteins were incubated with the corresponding secondary antibodies (1:2000 dilution) for 1 h at room temperature (BOSTER, USA). Quantification was performed on single channels with ImageJ software.

### *Statistics*

The results were presented as means  $\pm$  standard deviation (SD). The Student's *t*-test was applied to analyze differences between groups. Estimations are presented with 95% confidence intervals. Differences were considered significant at a *P*-value of <0.05. Statistical analysis was undertaken using SPSS and GraphPad Prism v.6 (GraphPad Software Inc., La Jolla, CA, USA).

## **Results**

### *Screening for differentially expressed circRNAs*

In the present study, next-generation sequencing was employed to identify differentially expressed circRNAs (DECs) between PTC tissue

and corresponding pericarcinomatous tissue. HE staining provided representative images of the three paired tissues (**Figure 1A**) and a hierarchical clustering method was then used to reveal the DECs after low-quality data were filtered out (**Figure 1B**). Scatter plots show the DECs in each pair of PTC and pericarcinomatous tissues (**Figure 1C**). A fold change method and the Student's *t*-test were applied to analyze DECs. A more detailed description of this processes is given in the Materials and Methods section. Using a back-spliced junction reads method, we found that 155, 17, and 17 DECs were significantly up-regulated in PTC tissues compared to pericarcinomatous tissues in three patients (patients HA, WA, and LA, respectively). Meanwhile, 153, 37, and 11 DECs, respectively, were significantly downregulated in PTC tissues compared to pericarcinomatous tissues.

To determine the role of circRNA in gene regulation, we performed GO analyses of biological processes, cellular components, and molecular functions, as shown in **Figure 2A-C**. The results of KEGG pathway analysis are presented in **Figure 2D-F**. The host genes of DECs were mainly associated with the PI3K/AKT signaling pathway, focal adhesion, and platelet activation.

In order to further confirm the RNA-seq result, the two circRNAs (hsa\_circ\_0000690 and hsa\_circ\_0006357) that were significantly upregulated and three circRNAs (hsa\_circ\_0000864, hsa\_circ\_0008797, and hsa\_circ\_0007694) that were down-regulated in PTC tissues compared to pericarcinomatous tissues were selected for qRT-PCR validation. The results (**Figure 2G**) showed that hsa\_hsa\_circ\_0007694, hsa\_circ\_0008797, and hsa\_circ\_0000864 were down-regulated in the PTC tissues (n=12), which is consistent with the RNA-seq results. However, the expression of hsa\_circ\_0000690 and hsa\_circ\_0006357 was not significantly different between tissues according to qRT-PCR.

*Verification of the functions of hsa\_hsa\_circ\_0007694 in cell proliferation, migration, invasion, and apoptosis*

Based on the results of qRT-PCR verification, hsa\_circ\_0007694 was selected for further analysis by agarose gel electrophoresis and

Sanger sequencing (**Figure 3A** and **3B**). While hsa\_circ\_0007694 produced bands of the expected sizes in cDNA analysis of PTC and pericarcinomatous tissues, these bands were not observed in gDNA analysis. The back-spliced junction sites were validated and we confirmed the expression levels of hsa\_circ\_0007694 in the PTC cell lines with qRT-PCR (**Figure 3C**).

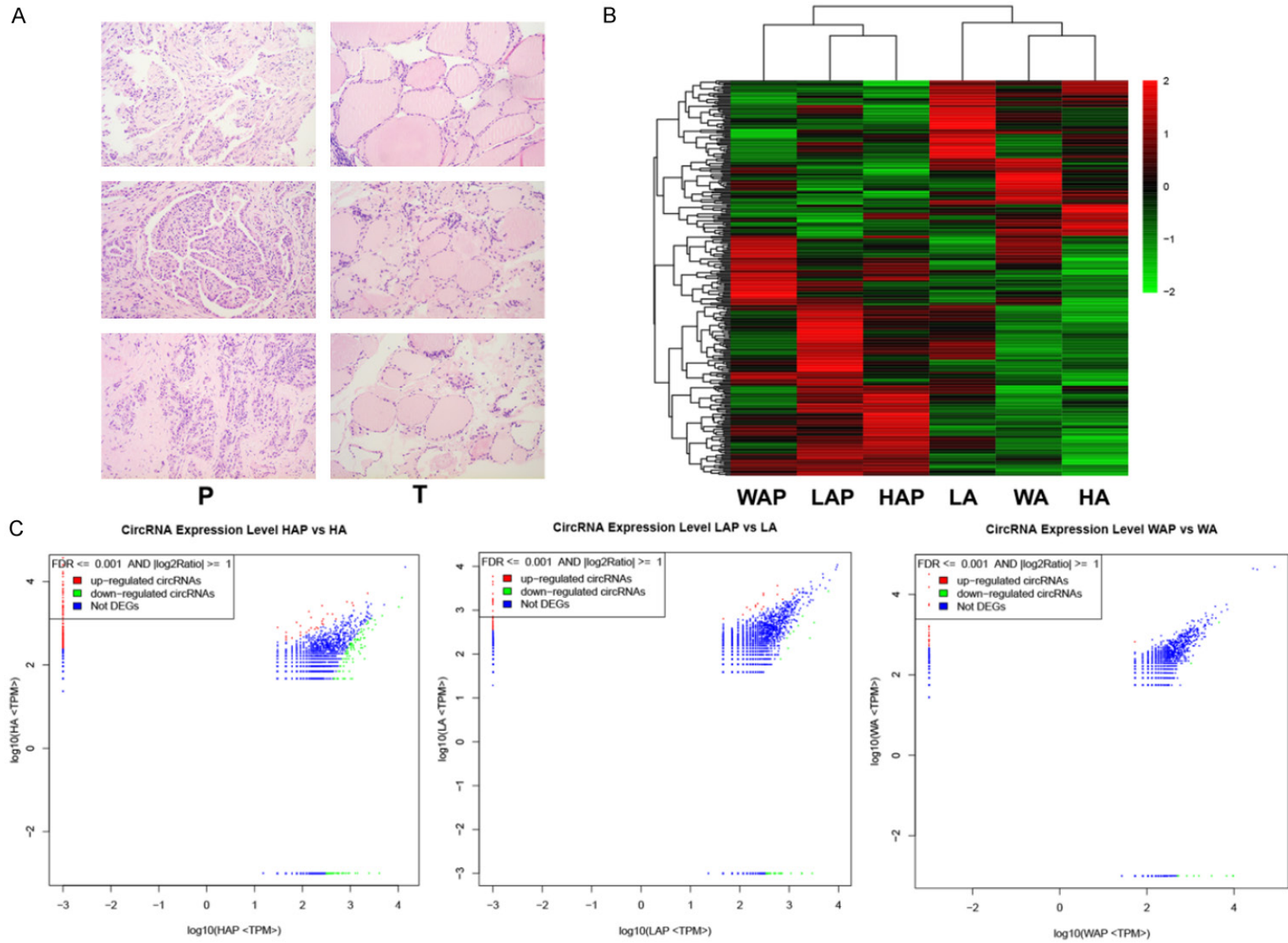
To investigate the role of hsa\_circ\_0007694, we constructed an over-expression system with a pEZ-LV003 vector to increase the expression of hsa\_circ\_0007694 in BHT-101 and KHM-5M cells. The results of qRT-PCR showed that hsa\_circ\_0007694 expression was significantly up-regulated after transfection (**Figure 3D**). Moreover, we tested whether over-expression of hsa\_circ\_0007694 in BHT-101 cell affected cell proliferation. MTT results showed that over-expression of hsa\_circ\_0007694 inhibited cell proliferation in both BHT-101 and KHM-5M cells (**Figure 3E**). The results of a cell colony formation assay were similar to those of the MTT assay. Cells transfected with the over-expression vector generated fewer colonies in both cell lines (**Figure 3F** and **3G**).

We then performed a transwell assay to check whether hsa\_circ\_0007694 regulates BHT-101 and KHM-5M cell migration and invasion. The results suggested that over-expression of hsa\_circ\_0007694 in BHT-101 and KHM-5M cells can effectively repress cell migration and invasion (**Figure 4A**). Further, we studied the effects of hsa\_circ\_0007694 over-expression on cell apoptosis and found that apoptosis was promoted in cells over-expressing this circRNA compared to mock vehicle cells ( $P < 0.01$ ) (**Figure 4B**). In addition, a cell cycle study revealed that over-expression of hsa\_circ\_0007694 in BHT-101 and KHM-5M cells promoted transient cell accumulation in S phase and decreased transient cell accumulation in G1 phase (**Figure 4C**), suggesting a block at S phase.

*Over-expression of hsa\_circ\_0007694 suppressed the growth of tumors in nude mice*

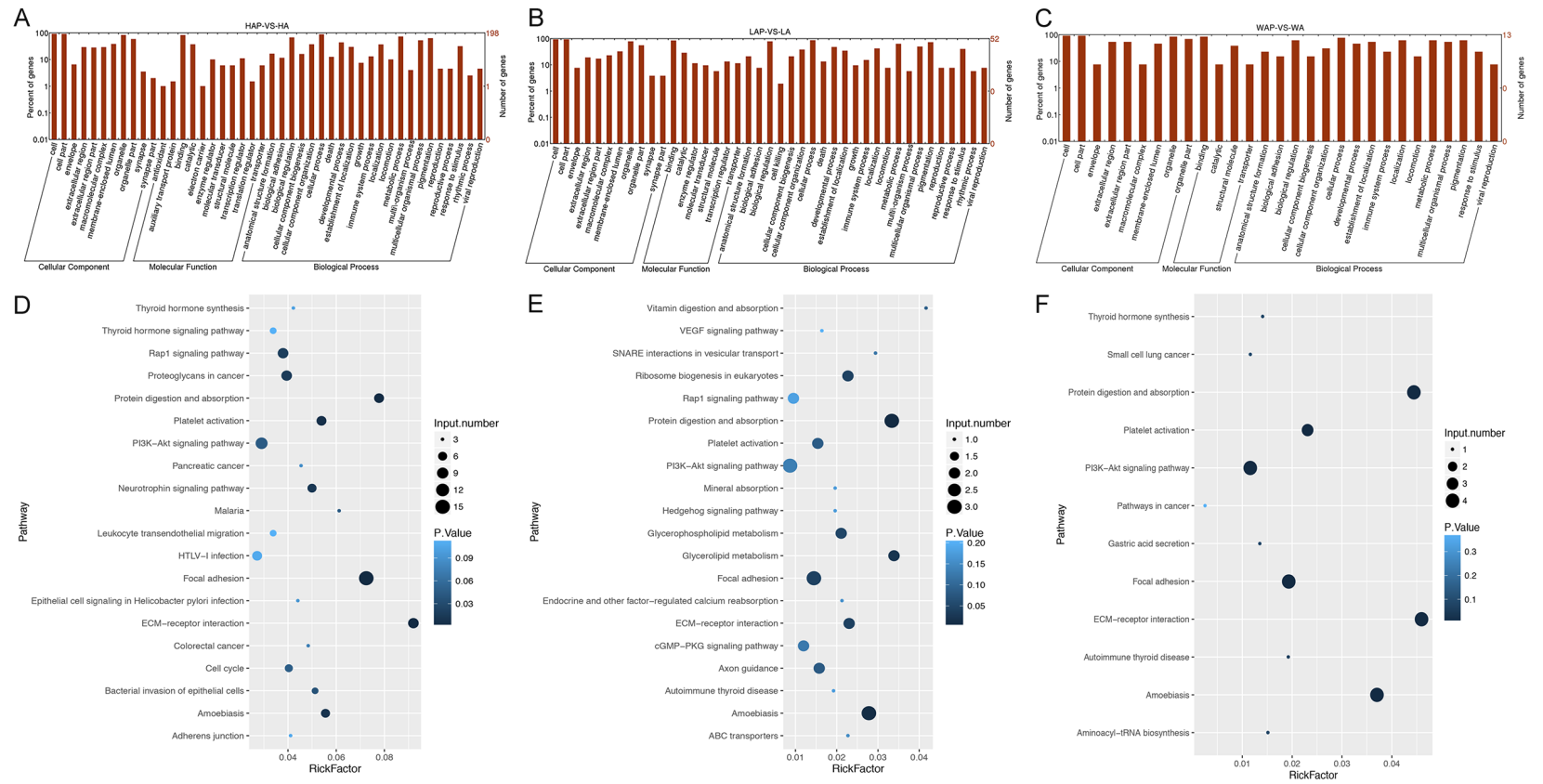
In order to study the effects of hsa\_circ\_0007694 over-expression in BHT-101 cells *in vivo*, both BHT-101 cells over-expressing hsa\_circ\_0007694 and BHT-101 cells treated with mock vehicle were injected subcutaneously

Role of hsa\_hsa\_circ\_0007694 in thyroid cancer



# Role of hsa\_hsa\_circ\_0007694 in thyroid cancer

**Figure 1.** Scatter plots and volcano plots that show differentially expressed circRNAs. A. Representative H&E-stained images of three PTC tumor samples (T) and paired pericarcinomatous samples (P). The samples were imaged at 100× magnifications. B. Hierarchical clustering analysis of differential circRNA expression between PTC tissues and pericarcinomatous tissues. C. Scatter plots used to identify differentially expressed circRNAs in PTC tumors versus normal thyroid tissue. HA and HAP, WA and WAP, LA and LAP represent the tumor tissue and paired pericarcinomatous tissue of patients HA, WA, and LA, respectively. Green indicates low expression of circRNA and red indicates high expression of circRNA.



Role of hsa\_hsa\_circ\_0007694 in thyroid cancer

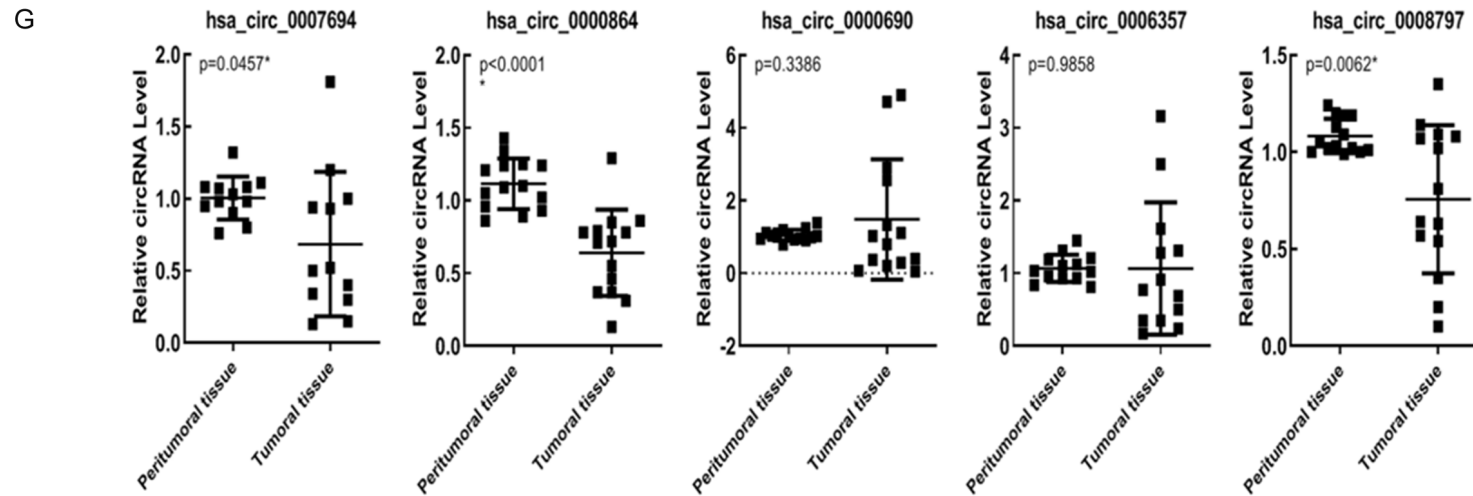
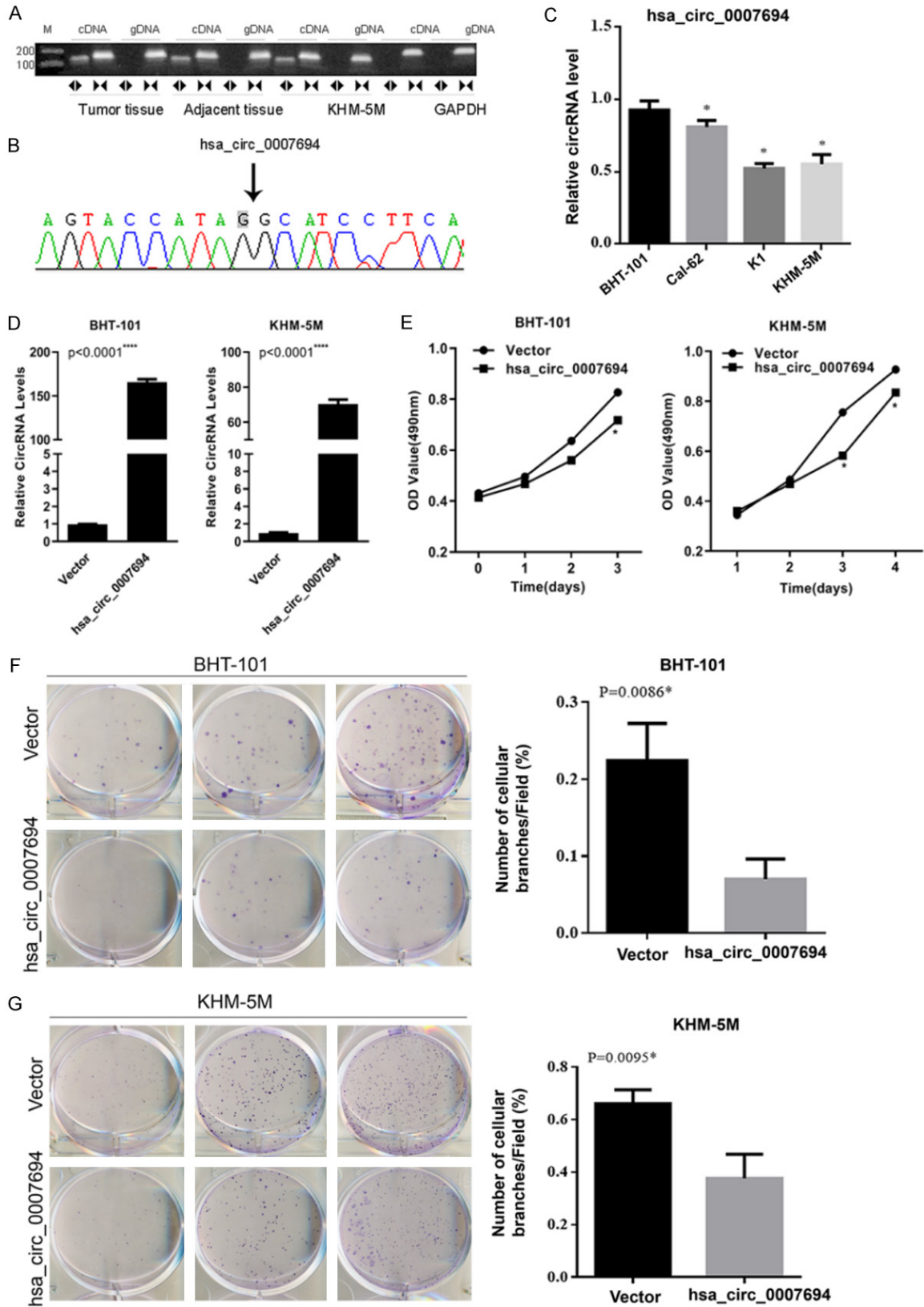


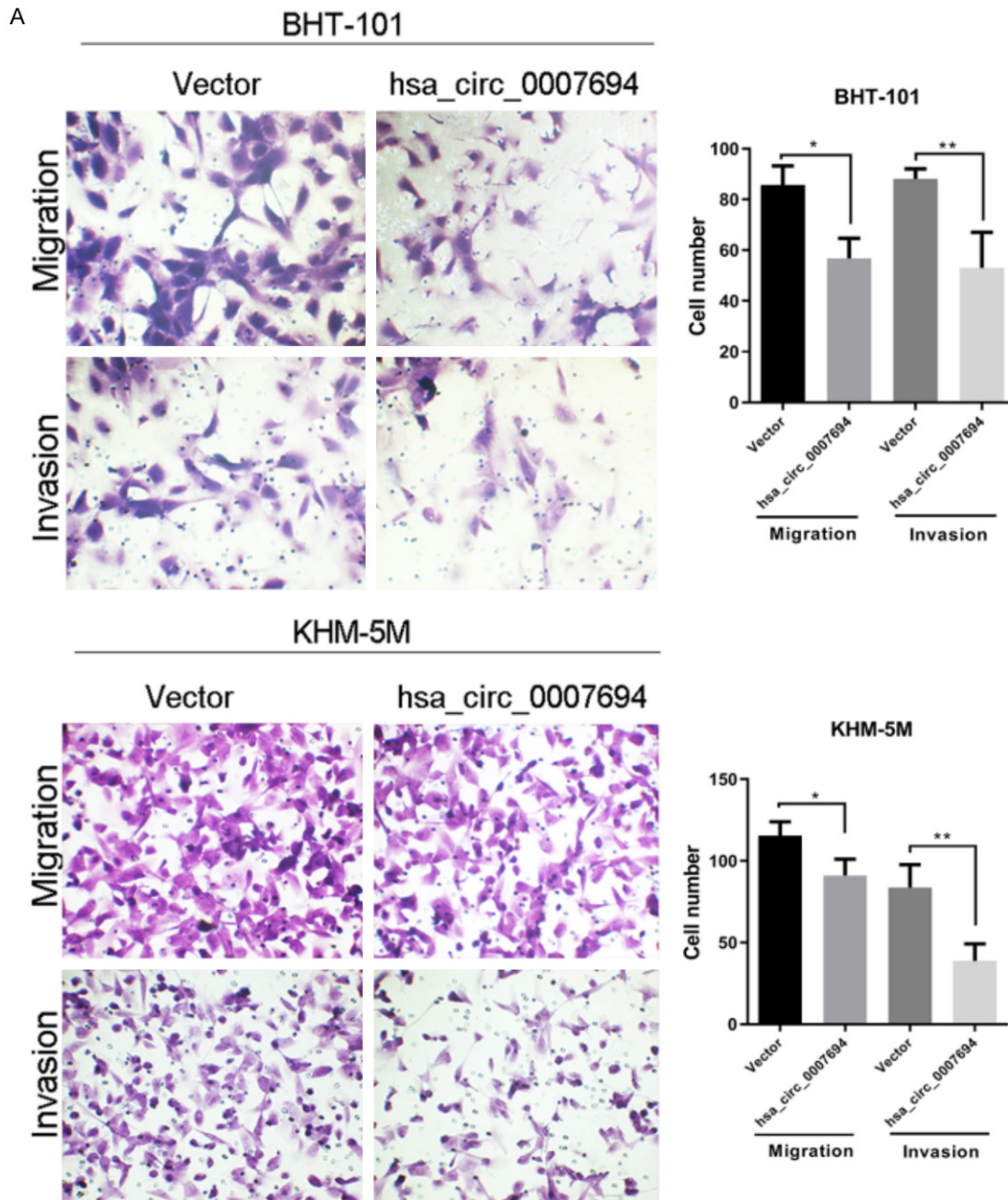
**Figure 2.** GO and KEGG analyses of the host genes of differentially expressed circRNAs and qRT-PCR validation of differential circRNAs. A-C. GO analyses of the genes that produce differentially expressed circRNA. D-F. KEGG pathway enrichment analyses of the genes that produce up-regulated and down-regulated circRNAs. G. qRT-PCR was used to validate the dysregulated expression of the two significantly up-regulated circRNAs and the three significantly down-regulated circRNAs. \*P<0.05.

# Role of hsa\_hsa\_circ\_0007694 in thyroid cancer

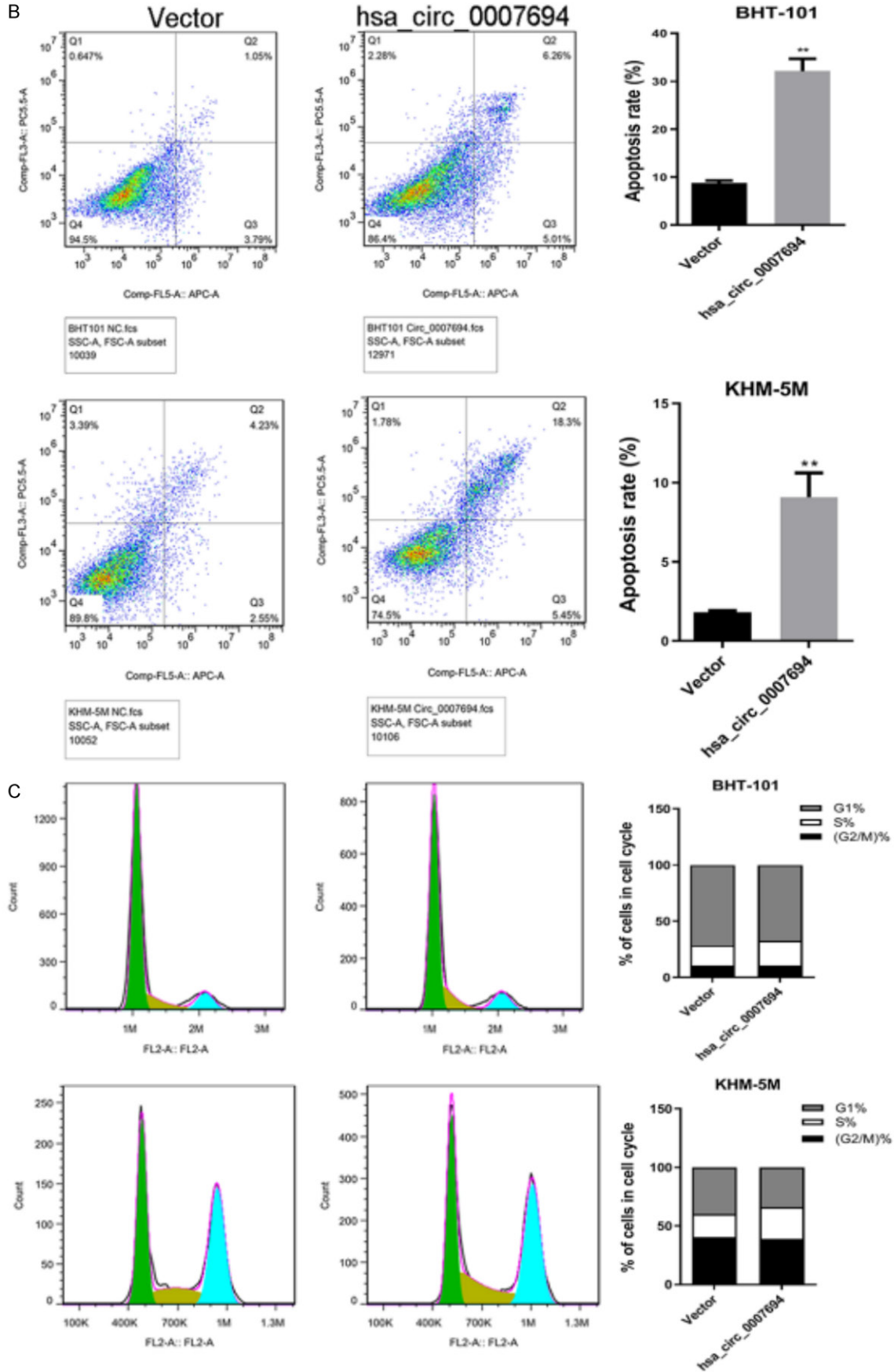


## Role of hsa\_hsa\_circ\_0007694 in thyroid cancer

**Figure 3.** hsa\_circ\_0007694 over-expression inhibited PTC cell proliferation. A. hsa\_circ\_0007694 was amplified by divergent primers with cDNA and gDNA from tumor tissue and paired pericarcinomatous tissue. circRNA could only be amplified from the cDNA template. M: DNA molecular markers. B. The head-to-tail back-splicing of hsa\_circ\_0007694 was confirmed by Sanger sequencing. The black arrow indicates the junction sequences of hsa\_circ\_0007694. C. qRT-PCR analysis of the hsa\_circ\_0007694 in PTC cell lines. D. qRT-PCR analysis of the effects of hsa\_circ\_0007694 transfection in BHT-101 and KHM-5M cells. E. Analysis of proliferation in BHT-101 and KHM-5M cells over-expressing hsa\_circ\_0007694 or treated with mock vector after 1, 2, and 3 d. F, G. Analysis of cell colony formation in BHT-101 and KHM-5M cells over-expressing hsa\_circ\_0007694 or treated with mock vector. \* $P < 0.05$ . \*\*\*\* $P < 0.0001$ .



Role of hsa\_hsa\_circ\_0007694 in thyroid cancer



## Role of hsa\_hsa\_circ\_0007694 in thyroid cancer

**Figure 4.** Over-expression of hsa\_circ\_0007694 inhibited migration and invasion and promoted apoptosis in PTC cells. A. Images of cell migration and invasion analysis of BHT-101 and KHM-5M cells over-expressing hsa\_circ\_0007694 or treated with mock vector. Samples were imaged at 40× magnification. B. Analysis of apoptosis in BHT-101 and KHM-5M cells over-expressing hsa\_circ\_0007694 or treated with mock vector. C. Analysis of cell cycle in BHT-101 and KHM-5M cells over-expressing hsa\_circ\_0007694 or treated with mock vector. \*P<0.05, \*\*P<0.01.

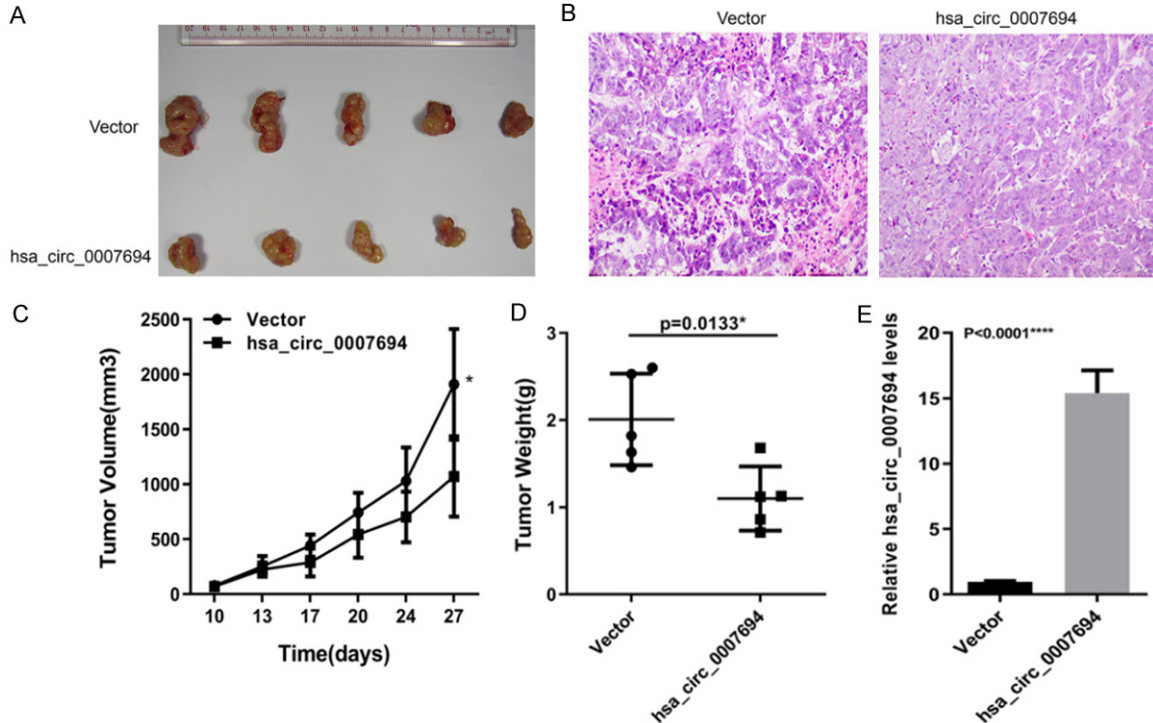


**Figure 5.** Over-expression of hsa\_circ\_0007694 suppressed the growth of tumors in nude mice. A. Images showing tumor volume 27 d after transplantation. B. Representative H&E-stained images of tumors derived from BHT-101 cells over-expressing hsa\_circ\_0007694 or treated with mock vector. C. Volumes of tumors derived from BHT-101 cells over-expressing hsa\_circ\_0007694 or treated with mock vector at five different time points. D. Weight of tumors derived from BHT-101 cells over-expressing hsa\_circ\_0007694 or treated with mock vector 27 d after transplantation. E. Expression of hsa\_circ\_0007694 in tumors derived from BHT-101 cells over-expressing hsa\_circ\_0007694 and mock vector tissues. \*P<0.05, \*\*\*\*P<0.0001.

into nude mice. The volume and weight of the tumors that developed from the different cells were recorded. After 27 d, the tumor weight was measured. **Figure 5A** shows the actual size of the tumors of five experimental animals. Additionally, we performed H&E staining to analyze the pathological characteristics of tumors obtained 27 d after injection (**Figure 5B**). **Figure 5C** shows that the tumor volume was lower in the hsa\_circ\_0007694 group compared to the mock vector group. The tumors that grew from cells over-expressing hsa\_circ\_0007694 were lighter than those that grew from mock vector-treated cells (**Figure 5D**). The results suggest that over-expression of hsa\_circ\_0007694 in BHT-101 cells could effectively inhibit tumor

growth. In addition, we analyzed the abundance of hsa\_circ\_0007694 in tumor and normal tissue harvested 27 d after injection by qRT-PCR. The results indicate that hsa\_circ\_0007694 was significantly up-regulated in tumor tissue compared to the mock vector group (**Figure 5E**).

### *Investigating the molecular mechanism of hsa\_circ\_0007694 in thyroid cancer*

In order to further study the molecular mechanisms related to hsa\_circ\_0007694, we performed transcriptome sequencing with BHT-101 cells over-expressing hsa\_circ\_0007694 and BHT-101 cells treated with mock vehicle.



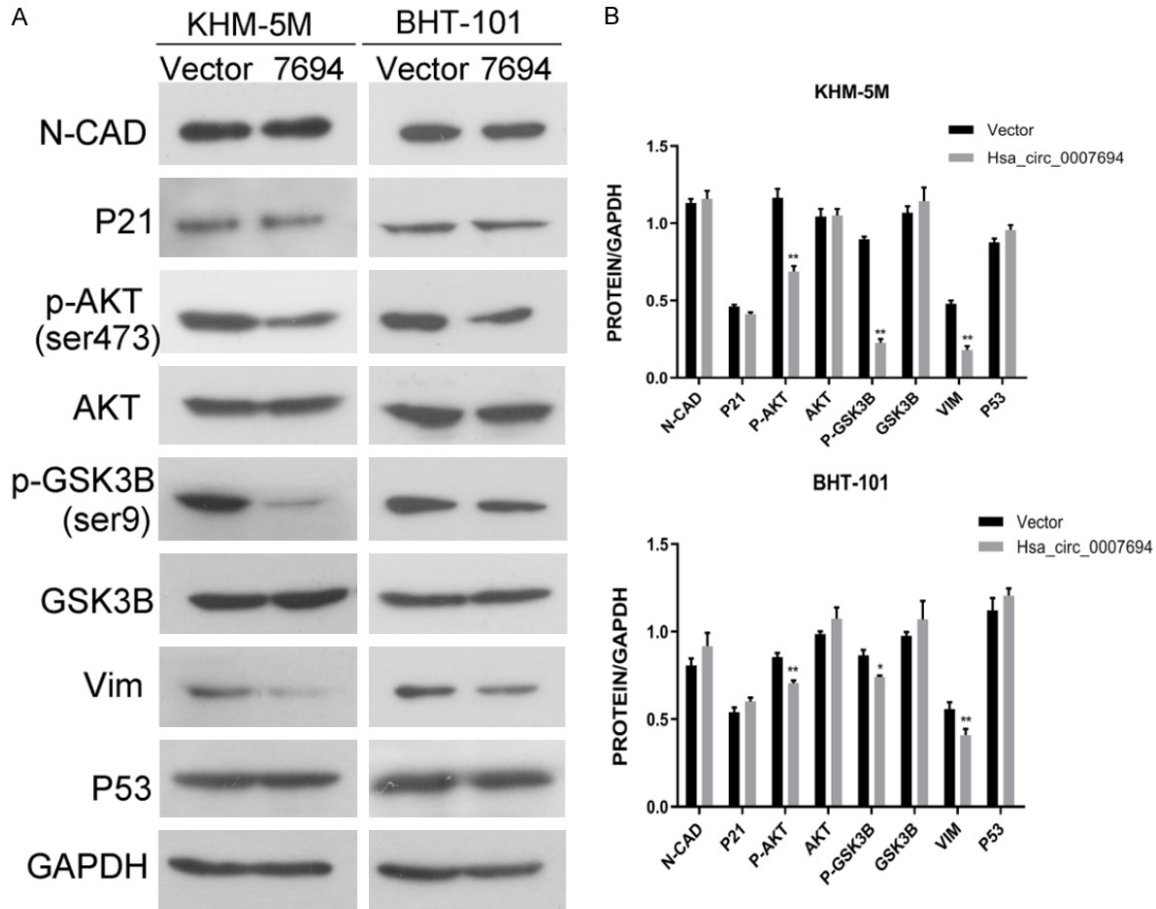


**Figure 7.** Western blot analysis of cancer-related proteins in BHT-101 cells and KHM-5M cells. Protein levels of N-CAD, p21, AKT, p-ATK<sup>Ser473</sup>, p-GSK3B<sup>Ser9</sup>, GSK3B, Vim, and p53 were detected by western blotting. “7694” indicates BHT-101 cells and KHM-5M cells over-expressing hsa\_circ\_0007694. \*P<0.05, \*\*P<0.01.

egory. Binding and catalytic activity were the top significantly overrepresented terms in the “molecular functions” category.

In the present study, we chose eight key proteins for KEGG analysis (N-CAD, p21, AKT, p-ATK<sup>Ser473</sup>, p-GSK3B<sup>Ser9</sup>, GSK3B, Vim, p53) to determine their expression levels in BHT-101 cells and KHM-5M cells over-expressing hsa\_circ\_0007694 or treated with mock vehicle by western blot (**Figure 7A** and **7B**). The results suggest that there were no differences in N-CAD, p21, and p53 expression between the cell groups. However, the expression of p-ATK<sup>Ser473</sup>, p-GSK3B<sup>Ser9</sup>, and Vim were significantly lower, and the levels of AKT and GSK3B were slightly lower in all cells over-expressing hsa\_circ\_0007694 than in all cells treated with mock vehicle. We speculate that over-expression of hsa\_circ\_0007694 in both cell types

could inhibit cell proliferation and migration via p-ATK<sup>Ser473</sup>, p-GSK3B<sup>Ser9</sup>, and Vim-related signaling pathways, including pathways related to cancer and the PI3K-AKT signaling pathway.

### Discussion

In the present study, numerous differentially expressed circRNAs (DECs) were identified between PTC tissues and pericarcinomatous tissues. Of these DECs, 155, 17, and 17 were significantly up-regulated in PTC tissues compared to pericarcinomatous tissues in three PTC patients. Meanwhile, 153, 37, and 11 DECs were significantly down-regulated in PTC tissues compared to pericarcinomatous tissues in the same three patients. These results suggest the differential expression of circRNAs in PTC tissues. The role of circRNA in the thyroid has previously been studied [18, 19]. Wei et al.

[20] and Pan et al. [21] showed that circZFR and circ\_0025033 were up-regulated in PTC tissues and promoted PTC cell proliferation and invasion. A study by Lan et al. suggested that hsa\_circ\_0137287 could predict the clinicopathologic characteristics of PTC [22]. These results confirm that it is necessary to study the function of circRNA in thyroid cancer, as such research could provide guidance for the diagnosis and prediction of prognosis of thyroid cancer.

In the present study, hsa\_circ\_0007694 was found to be significantly down-regulated in thyroid lesions compared to pericarcinomatous tissues, and this was confirmed by qRT-PCR. It is reported that hsa\_circ\_0007694 was first found to be enriched in ALU repeats in human T lymphocytes and telomerized Hs68 human fibroblast cells [23]. Subsequently, this molecule was identified in various cell lines and the cerebellum [24, 25]. However, there is still little available information relating to the roles of hsa\_circ\_0007694 in cancer, especially thyroid cancer. Therefore, we constructed a hsa\_circ\_0007694 over-expression system to study its functions in thyroid cancer cell lines. Over-expression of hsa\_circ\_0007694 promoted apoptosis and inhibited proliferation, migration, and invasion in BHT-101 and KHM-5M cells. These findings suggest that over-expression of hsa\_circ\_0007694 could effectively restrict cell behaviors. Based on the evidence mentioned above, we speculate that hsa\_circ\_0007694 is a multifunctional molecule that could be related to multiple signaling pathways related to cell proliferation, behaviors, apoptosis, etc. In the present study, we also investigated the effects of hsa\_circ\_0007694 in *in vivo* mouse models. We found that cells over-expressing hsa\_circ\_0007694 produced tumors that were lower in size and weight; these tumors were subsequently excised for further study. In addition, we performed RNA-seq to study, in detail, the molecular mechanisms of hsa\_circ\_0007694 in BHT-101 cells. GO enrichment analysis indicated that cellular processes, biological regulation, cells, cell parts, and binding were the most enriched terms. These diverse functions indirectly reveal that hsa\_circ\_0007694 is a multipotent molecule.

KEGG analysis indicated that the PI3K/AKT/mTOR signaling pathway was enriched in this

study, and this was verified by western blot. The results showed that in cells over-expressing hsa\_circ\_0007694, the protein expression of p-ATK<sup>Ser473</sup>, p-GSK3B<sup>Ser9</sup>, and Vim were significantly decreased, which indicates that hsa\_circ\_0007694 over-expression could inhibit cell proliferation and migration via the PI3K/AKT/mTOR signaling pathway. This pathway is activated in many types of cancer, such as breast cancer, renal cell cancer, non-small cell lung cancer, gastroesophageal cancer, and hepatocellular cancer [26]. A previous cell apoptosis study indicated that the PI3K/AKT/mTOR signaling pathway could inhibit cell apoptosis via the phosphorylation of Ser196 in caspase-3 and caspase-9 by activated AKT [27]. Additionally, a tumor metastasis study suggested that the PI3K/AKT pathway could up-regulate the mRNA and protein abundance of MMP2/MMP9, which could increase tumor cell metastasis and invasion [28, 29]. In summary, PI3K/Akt/mTOR plays an important role in tumor cells. Based on the above, we speculate that the anticancer effects of hsa\_circ\_0007694 may manifest via the PI3K/AKT/mTOR signaling pathway. Additionally, the Wnt signaling pathway was enriched in the present study. The Wnt signaling pathway has been linked to various types of cancer, including colorectal cancer, gastric cancer, lung cancer, cervical cancer, and malignant melanoma [30]. The detailed mechanisms of the Wnt signaling pathway are divergent in different cancer types. In thyroid cancer, the Wnt pathway mainly functions by activating downstream  $\beta$ -catenin [31]. Therefore, we speculate that hsa\_circ\_0007694 may regulate the Wnt pathway in thyroid cancer, but the detail of the mechanisms by which this occurs still need to be studied.

In the present study, we screened and identified hsa\_circ\_0007694 as the most differentially expressed circRNA in thyroid cancer tissue. A cell function study suggested that over-expression of hsa\_circ\_0007694 effectively inhibits cell behaviors and tumor growth *in vitro* and *in vivo*. Transcriptome sequencing analysis revealed that the PI3K/AKT/mTOR and Wnt signaling pathways are potential hsa\_circ\_0007694-related pathways. Therefore, hsa\_circ\_0007694 plays an important role in thyroid cancer. This molecule may be valuable in future clinical applications.

**Acknowledgements**

This study was supported by the Natural Science Foundation of Guangdong Province (2018A030313837).

**Disclosure of conflict of interest**

None.

**Address correspondence to:** Lang-Ping Tan and Hong-Hao Li, Department of Thyroid Surgery, Sun Yat-sen Memorial Hospital, Sun Yat-sen University, No. 107 Yanjiang West Road, Yuexiu District, Guangzhou 510000, China. Tel: +86-20-34070219; Fax: +86-20-81332199; E-mail: tanlp7@mail.sysu.edu.cn (LPT); lihh8@163.com (HHL)

**References**

[1] Siegel R, Naishadham D and Jemal A. Cancer statistics, 2013. *CA Cancer J Clin* 2013; 63: 11-30.

[2] Haugen BR, Alexander EK, Bible KC, Doherty GM, Mandel SJ, Nikiforov YE, Pacini F, Randolph GW, Sawka AM, Schlumberger M, Schuff KG, Sherman SI, Sosa JA, Steward DL, Tuttle RM and Wartofsky L. 2015 American Thyroid Association management guidelines for adult patients with thyroid nodules and differentiated thyroid cancer: the American Thyroid Association guidelines task force on thyroid nodules and differentiated thyroid cancer. *Thyroid* 2016; 26: 1-133.

[3] Sampson E, Brierley JD, Le LW, Rotstein L and Tsang RW. Clinical management and outcome of papillary and follicular (differentiated) thyroid cancer presenting with distant metastasis at diagnosis. *Cancer* 2007; 110: 1451-1456.

[4] Gupta M, Gupta S and Gupta VB. Correlation of fine needle aspiration cytology with histopathology in the diagnosis of solitary thyroid nodule. *J Thyroid Res* 2010; 2010: 379051.

[5] Cibas ES and Ali SZ. The Bethesda system for reporting thyroid cytopathology. *Am J Clin Pathol* 2009; 132: 658-665.

[6] Yip L. Molecular markers for thyroid cancer diagnosis, prognosis, and targeted therapy. *J Surg Oncol* 2015; 111: 43-50.

[7] Li F, Chen G, Sheng C, Gusdon AM, Huang Y, Lv Z, Xu H, Xing M and Qu S. BRAFV600E mutation in papillary thyroid microcarcinoma: a meta-analysis. *Endocr Relat Cancer* 2015; 22: 159-168.

[8] Kim TH, Park YJ, Lim JA, Ahn HY, Lee EK, Lee YJ, Kim KW, Hahn SK, Youn YK, Kim KH, Cho BY and Park DJ. The association of the BRAF(V600E) mutation with prognostic factors

and poor clinical outcome in papillary thyroid cancer: a meta-analysis. *Cancer* 2012; 118: 1764-1773.

[9] An S and Song JJ. The coded functions of non-coding RNAs for gene regulation. *Mol Cells* 2011; 31: 491-496.

[10] Anastasiadou E, Jacob LS and Slack FJ. Non-coding RNA networks in cancer. *Nat Rev Cancer* 2018; 18: 5-18.

[11] Memczak S, Jens M, Elefsinioti A, Torti F, Krueger J, Rybak A, Maier L, Mackowiak SD, Gregersen LH and Munschauer M. Circular RNAs are a large class of animal RNAs with regulatory potency. *Nature* 2013; 495: 333-8.

[12] Zhang Y, Zhang XO, Chen T, Xiang JF, Yin QF, Xing YH, Zhu S, Yang L and Chen LL. Circular intronic long noncoding RNAs. *Mol Cell* 2013; 51: 792-806.

[13] Bachmayr-Heyda A, Reiner AT, Auer K, Sukhbaatar N, Aust S, Bachleitner-Hofmann T, Mesteri I, Grunt TW, Zeillinger R and Pils D. Correlation of circular RNA abundance with proliferation-exemplified with colorectal and ovarian cancer, idiopathic lung fibrosis, and normal human tissues. *Sci Rep* 2015; 5: 8057.

[14] Wang Y and Wang Z. Efficient backsplicing produces translatable circular mRNAs. *RNA* 2015; 21: 172-179.

[15] Zhao W, Cheng Y, Zhang C, You Q, Shen X, Guo W and Jiao Y. Genome-wide identification and characterization of circular RNAs by high throughput sequencing in soybean. *Sci Rep* 2017; 7: 5636.

[16] Lin L, Park JW, Ramachandran S, Zhang Y, Tseng YT, Shen S, Waldvogel HJ, Curtis MA, Faull RL, Troncoso JC, Pletnikova O, Ross CA, Davidson BL and Xing Y. Transcriptome sequencing reveals aberrant alternative splicing in Huntington's disease. *Hum Mol Genet* 2016; 25: 3454-3466.

[17] Xie C, Mao X, Huang J, Ding Y, Wu J, Dong S, Kong L, Gao G, Li CY and Wei L. KOBAS 2.0: a web server for annotation and identification of enriched pathways and diseases. *Nucleic Acids Res* 2011; 39: W316-W322.

[18] Peng N, Shi L, Zhang Q, Hu Y, Wang N and Ye H. Microarray profiling of circular RNAs in human papillary thyroid carcinoma. *PLoS One* 2017; 12: e0170287.

[19] Lan X, Xu J, Chen C, Zheng C, Wang J, Cao J, Zhu X and Ge M. The landscape of circular RNA expression profiles in papillary thyroid carcinoma based on RNA sequencing. *Cell Physiol Biochem* 2018; 47: 1122-1132.

[20] Wei H, Pan L, Tao D and Li R. Circular RNA circ-ZFR contributes to papillary thyroid cancer cell proliferation and invasion by sponging miR-1261 and facilitating C8orf4 expression. *Bio-*

## Role of hsa\_hsa\_circ\_0007694 in thyroid cancer

- chem Biophys Res Commun 2018; 503: 56-61.
- [21] Pan Y, Xu T, Liu Y, Li W and Zhang W. Upregulated circular RNA circ\_0025033 promotes papillary thyroid cancer cell proliferation and invasion via sponging miR-1231 and miR-1304. *Biochem Biophys Res Commun* 2019; 510: 334-338.
- [22] Lan X, Cao J, Xu J, Chen C, Zheng C, Wang J, Zhu X, Zhu X and Ge M. Decreased expression of hsa\_circ\_0137287 predicts aggressive clinicopathologic characteristics in papillary thyroid carcinoma. *J Clin Lab Anal* 2018; 32: e22573.
- [23] Jeck WR, Sorrentino JA, Wang K, Slevin MK, Burd CE, Liu J, Marzluff WF and Sharpless NE. Circular RNAs are abundant, conserved, and associated with ALU repeats. *RNA* 2013; 19: 141-157.
- [24] Salzman J, Chen RE, Olsen MN, Wang PL and Brown PO. Cell-type specific features of circular RNA expression. *PLoS Genet* 2013; 9: e1003777.
- [25] Rybak-Wolf A, Stottmeister C, Glázar P, Jens M, Pino N, Giusti S, Hanan M, Behm M, Bartok O, Ashwal-Fluss R, Herzog M, Schreyer L, Papavasileiou P, Ivanov A, Öhman M, Refojo D, Kadener S and Rajewsky N. Circular RNAs in the mammalian brain are highly abundant, conserved, and dynamically expressed. *Mol Cell* 2015; 58: 870-885.
- [26] Xia P and Xu XY. PI3K/Akt/mTOR signaling pathway in cancer stem cells: from basic research to clinical application. *Am J Cancer Res* 2015; 5: 1602-9.
- [27] Henshall DC, Araki T, Schindler CK, Lan JQ, Tiekoter KL, Taki W and Simon RP. Activation of Bcl-2-associated death protein and counter-response of Akt within cell populations during seizure-induced neuronal death. *J Neurosci* 2002; 22: 8458-8465.
- [28] Chien CS, Shen KH, Huang JS, Ko SC and Shih YW. Antimetastatic potential of fisetin involves inactivation of the PI3K/Akt and JNK signaling pathways with downregulation of MMP-2/9 expressions in prostate cancer PC-3 cells. *Mol Cell Biochem* 2010; 333: 169-80.
- [29] Gao Y, Guan Z, Chen J, Xie H, Yang Z, Fan J, Wang X and Li L. CXCL5/CXCR2 axis promotes bladder cancer cell migration and invasion by activating PI3K/AKT-induced upregulation of MMP2/MMP9. *Int J Oncol* 2015; 47: 690-700.
- [30] Zhang X and Hao J. Development of anticancer agents targeting the Wnt/ $\beta$ -catenin signaling. *Am J Cancer Res* 2015; 5: 2344-60.
- [31] Sastre-Perona A and Santisteban P. Role of the wnt pathway in thyroid cancer. *Front Endocrinol (Lausanne)* 2012; 3: 31.